ORGANIC LETTERS

2012
Vol. 14, No. 20
5226–5229

Large Stokes Shift Induced by Intramolcular Charge Transfer in N,O-Chelated Naphthyridine–BF_2 Complexes

Yun-Ying Wu,[†,‡] Yong Chen,[*,‡] Gao-Zhang Gou,[†] Wei-Hua Mu,[†] Xiao-Jun Lv,[‡] Mei-Ling Du,[†] and Wen-Fu Fu[*,†,‡]

College of Chemistry and Chemical Engineering, Yunnan Normal University, Kunming 650092, P.R. China, and Key Laboratory of Photochemical Conversion and Optoelectronic Materials, CAS-HKU Joint Laboratory on New Materials, Technical Institute of Physics and Chemistry, Chinese Academy of Sciences, Beijing 100190, P.R. China

fuwf@mail.ipc.ac.cn; chenyong@mail.ipc.ac.cn

Received August 22, 2012

ABSTRACT

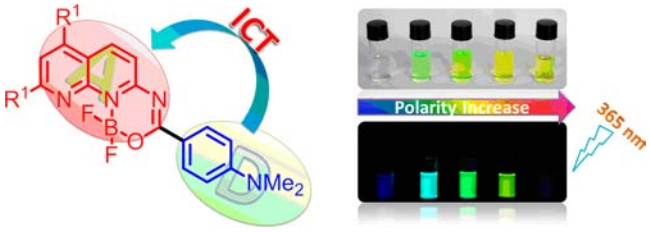

Novel N,O-chelated naphthyridine–BF_2 complexes with push–pull structures have been synthesized and characterized. Spectral investigations on these complexes reveal that photoinduced intramolecular charge transfer occurs and results in a large Stokes shift, which is further supported by density functional theory based theoretical calculations.

The notable advantages of borondipyrromethene (BODIPY) derivatives, such as high extinction coefficients and intense fluorescence emissions ranging from the blue to near-infrared (NIR) region, are crucially responsible for enabling them to have potential use in a wide range of applications involving light harvesting, energy transport, sensing, or biological imaging.[1] Unfortunately, the intense fluorescence of BODIPY dyes in the solution phase is usually quenched in the solid state because of intermolecular interactions (e.g., $\pi-\pi$ stacking).[2] Moreover, most luminescent BODIPY derivatives display to a limited extent a Stokes shift (<20 nm), which results in self-absorption of the higher energy part of their emission spectra and in measurement interference by excitation light and scattered light. Tremendous efforts have been directed toward addressing this issue, and considerable progress has been achieved in this context. For example, Piers et al. explored high Stokes shift anilido-pyridine BF_2 dyes by harnessing a desymmetrized ligand to render the ground and excited states more energetically distinct.[3] Bulky side substituents have been introduced into BODIPY dyes to enlarge the Stokes shift and also to reduce the $\pi-\pi$ stacking in the solid state.[4] A large pseudo-Stokes shift has also been realized by fluorescence resonance

[†] Yunnan Normal University.
[‡] Chinese Academy of Sciences.

(1) (a) Loudet, A.; Burgess, K. *Chem. Rev.* **2007**, *107*, 4891–4932. (b) Ziessel, R.; Ulrich, G.; Harriman, A. *New J. Chem.* **2007**, *31*, 496–501. (c) Ulrich, G.; Ziessel, R.; Harriman, A. *Angew. Chem., Int. Ed.* **2008**, *47*, 1184–1201.

(2) (a) Birks, J. B. *Photophysics of Aromatic Molecules*; Wiley-Interscience: London, 1970. (b) Hong, Y.; Lam, J. W. Y.; Tang, B. Z. *Chem. Soc. Rev.* **2011**, *40*, 5361–5388. (c) Yang, Y.; Su, X.; Carroll, C. N.; Aprahamian, I. *Chem. Sci.* **2012**, *3*, 610–613.

(3) Araneda, J. F.; Piers, W. E.; Heyne, B.; Parvez, M.; McDonald, R. *Angew. Chem., Int. Ed.* **2011**, *50*, 12214–12217.

(4) (a) Zhang, D.; Wen, Y.; Xiao, Y.; Yu, G.; Liu, Y.; Qian, X. *Chem. Commun.* **2008**, 4777–4779. (b) Vu, T. T.; Badré, S.; Dumas-Verdes, C.; Vachon, J.-J.; Julien, C.; Audebert, P.; Senotrusova, E. Y.; Schmidt, E. Y.; Trofimov, B. A.; Pansu, R. B.; Clavier, G.; Méallet-Renault, R. *J. Phys. Chem. C* **2009**, *113*, 11844–11855. (c) Ozdemir, T.; Atilgan, S.; Kutuk, I.; Yildirim, L. T.; Tulek, A.; Bayindir, M.; Akkaya, E. U. *Org. Lett.* **2009**, *11*, 2105–2107. (d) Fu, G.-L.; Pan, H.; Zhao, Y.-H.; Zhao, C.-H. *Org. Biomol. Chem.* **2011**, *9*, 8141–8146. (e) Lu, H.; Wang, Q.; Gai, L.; Li, Z.; Deng, Y.; Xiao, X.; Lai, G.; Shen, Z. *Chem.—Eur. J.* **2012**, *18*, 7852–7861.

10.1021/ol302347m
Published on Web 10/10/2012

energy transfer (FRET)[5] and through-bond energy transfer (TBET).[6] While photoinduced intramolecular charge transfer (ICT) has been utilized with the aim of achieving a large Stokes shift in common organic systems, this strategy has rarely been adopted in BODIPYs and their analogues.[7]

We are interested in the design and synthesis of naphthyridine-based BF_2 complexes with intriguing luminescence properties. Previously, we reported a bis(BF_2) core complex containing 1,8-naphthyridine units; the complex displayed a yellow-green emission with a fluorescence quantum yield up to 0.965 in dichloromethane.[8] Similar to most BODIPYs and their analogues, this naphthyridine–BF_2 complex exhibited faint photoluminescence in the solid state. By controlling the molecular arrangements and the number of $\pi-\pi$ interactions in the solid state, we then successfully obtained solid-state emissive 1,8-naphthyridine–BF_2 complexes.[9] One significant deficit in the properties of these dyes is their generally small Stokes shift. In the present work, we propose to develop solid-emissive 1,8-naphthyridine–BF_2 complexes with large Stokes shifts. Our strategy involves the incorporation of an electron-donating dimethylamino aryl group into the 1,8-naphthyridine–BF_2 moiety, which is anticipated to result in a push–pull system in view of the fact that the naphthyridine unit is a well-known acceptor. Indeed, the newly synthesized donor–acceptor compounds (Scheme 1) were found to exhibit efficient intramolecular charge-transfer (ICT) emission in polar solvents with relatively large Stokes shifts and strong solvatochromism. For comparison, complexes **3b** and **4b** with a relatively neutral group (H for **3b**) or an electron-withdrawing group (COOMe for **4b**) on the *p*-position of the phenyl ring have also been prepared.

Scheme 1. Synthetic Routes and Chemical Structures of **1b**–**4b**

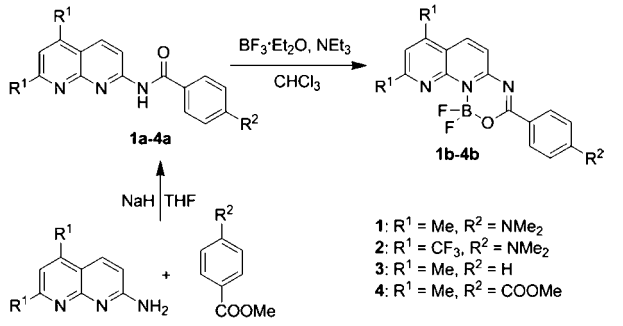

As shown in Scheme 1, the naphthyridine–BF_2 compounds were successfully obtained by a facile two-step synthetic route starting from 2-amino-5,7-dimethyl-1,8-naphthyridine or 2-amino-5,7-di(trifluoromethyl)-1,8-naphthyridine.[10] The raw materials were converted to **1a**–**4a** by reacting with *p*-substituted methyl benzoate in dry THF with sodium hydride as a base; the resulting amido ligands were treated with $BF_3 \cdot Et_2O$ in dry chloroform in the presence of triethylamine at rt to afford the desired fluorine–boron complexes **1b**–**4b** in high yields. All compounds synthesized were fully characterized by multinuclear NMR spectroscopy, ESI-MS, infrared spectroscopy, and elemental analyses. It is notable that the strong IR absorption peaks at ~1700 cm^{-1}, related to the C=O stretch vibration of the precursors **1a**–**4a**, vanished after coordination with BF_3 (Figure S1). Details of the experimental procedures and data for structural characterization were described in the Supporting Information (SI).

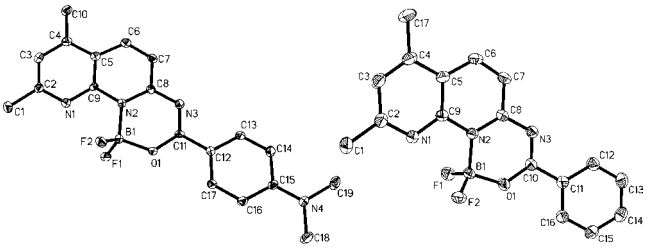

Figure 1. ORTEP diagrams for **1b** (left) and **3b** (right) showing 30% probability ellipsoids. All H-atoms are omitted for clarity.

Single crystals of complexes **1b**, **2b**, and **3b** suitable for X-ray diffraction analysis were grown by slow diffusion of diethyl ether vapors into a dichloromethane solution. Single crystals of the precursor **3a** and **4a** were also obtained by evaporating their dichloromethane solutions at rt. Detailed crystallographic data were summarized in Table S1.

Complex **1b** crystallizes in an orthorhombic lattice without solvates. The central B-atom has a slightly distorted tetrahedron geometry with B–F, B–N, B–O distances of 1.3795(2), 1.579(3), 1.471(3) Å, respectively, and bond angles around the B-atom ranging from 107.36(1)° to 112.47(2)°. These values for bond lengths and bond angles are normal for N,O-chelated BF_2 complexes.[11] As depicted in Figures 1 and S2, the entire molecule of **1b** is near coplanar, and all portions except for two F-atoms are located in the same plane; this suggests the formation of an extended π-conjugation system and is favorable for intramolecular charge transfer. The $\pi-\pi$ stacking interactions were found to exist along the

(5) (a) Coskun, A.; Akkaya, E. U. *J. Am. Chem. Soc.* **2005**, *127*, 10464–10465. (b) Coskun, A.; Akkaya, E. U. *J. Am. Chem. Soc.* **2006**, *128*, 14474–14475. (c) Belman, N.; Israelachvili, J. N.; Li, Y.; Safinya, C. R.; Bernstein, J.; Golan, Y. *J. Am. Chem. Soc.* **2009**, *131*, 9007–9013. (d) Harriman, A.; Mallon, L. J.; Elliot, K. J.; Haefele, A.; Ulrich, G.; Ziessel, R. *J. Am. Chem. Soc.* **2009**, *131*, 13375–13386. (e) Ziessel, R.; Rihn, S.; Harriman, A. *Chem.—Eur. J.* **2010**, *16*, 11942–11953. (f) Ziessel, R.; Harriman, A. *Chem. Commun.* **2011**, *47*, 611–631.

(6) (a) Zhao, Y.; Zhang, Y.; Lv, X.; Liu, Y.; Chen, M.; Wang, P.; Liu, J.; Guo, W. *J. Mater. Chem.* **2011**, *21*, 13168–13171. (b) Qu, X.; Liu, Q.; Ji, X.; Chen, H.; Zhou, Z.; Shen, Z. *Chem. Commun.* **2012**, *48*, 4600–4602.

(7) (a) Peng, X.; Song, F.; Lu, E.; Wang, Y.; Zhou, W.; Fan, J.; Gao, Y. *J. Am. Chem. Soc.* **2005**, *127*, 4170–4171. (b) Zhou, Y.; Xiao, Y.; Chi, S.; Qian, X. *Org. Lett.* **2008**, *10*, 633–636. (c) Frath, D.; Azizi, S.; Ulrich, G.; Retailleau, P.; Ziessel, R. *Org. Lett.* **2011**, *13*, 3414–3417. (d) Martin, A.; Long, C.; Forster, R. J.; Keyes, T. E. *Chem. Commun.* **2012**, *48*, 5617–5619.

(8) Li, H. F. J.; Fu, W. F.; Li, L.; Gan, X.; Mu, W. H.; Chen, W. Q.; Duan, X. M.; Song, H. B. *Org. Lett.* **2010**, *12*, 2924–2927.

(9) Quan, L.; Chen, Y.; Lv, X. J.; Fu, W. F. *Chem.—Eur. J.* **2012** DOI: 10.1002/chem.201201592.

(10) Henry, R. A.; Hammond, P. R. *J. Heterocycl. Chem.* **1977**, *14*, 1109–1112.

(11) Hachiya, S.; Inagaki, T.; Hashizume, D.; Maki, S.; Niwa, H.; Hirano, T. *Tetrahedron Lett.* **2010**, *51*, 1613–1615.

crystallographic *b*-axis direction, with a uniform intermolecular distance of 3.429 Å. For **2b**, the bulky CF_3 groups decorated on the naphthyridine ring lead to a slightly less planar molecular structure and a change in packing modes in the solid state (Figure S3).

Complex **3b** crystallizes into a pale yellow plate with a space group of *C*2/*c*. The crystal structure of **3b** reveals a nonplanar conformation; the dihedral angle between the naphthyridyl unit and the phenyl ring is 13.83°, which is comparable to that of 14.98° in its precursor. The striking difference between **3b** and **3a** is the bond parameters of the amido group (Figure S4 and Table S2). The C(10)—O(1) bond length of 1.3039(2) Å in **3b** is significantly longer with respect to that of 1.2242(2) Å in **3a**, but close to a typical C—O single bond (*ca.* 1.34 Å). In the meantime, the C(10)—N(3) bond distance of 1.3000(2) Å, characteristic of a C=N double bond, is pronouncedly shorter than that of 1.368(2) Å in its precursor. These results, coupled with IR observations, indicated a transformation from the keto to enol forms on changing from **3a** to **3b**.

The absorption and emission spectra of complexes **1b**–**4b** were measured in various solvents; the results are demonstrated in Figure S5, and the photophysical data are collected in Table 1. In general, the electron-donating substituent (NMe_2) at the phenyl *p*-position induced a remarkable red shift of the absorption maximum. As shown in Figure 2, complexes **3b** and **4b** in dichloromethane exhibit a structured absorption at 300–400 nm with a large extinction coefficient ($\sim 10^4$ mol^{-1} dm^3 cm^{-1}), which is typical for BF_2 compounds. In sharp contrast, complexes **1b** and **2b** display a broad and bathochromic absorption with λ_{max} at 440 and 480 nm, respectively. The red-shifted absorption of **1b** and **2b** can be attributed to originate from an ICT state, in terms of their strong push–pull structures.[12] Relative to **3b** and **4b**, large solvatochromic shifts are observed for **1b** and **2b**, indicative of the larger difference in dipole moments of the Franck–Condon (FC) excited state and the ground state in the latter.

The emission spectra of **1b** and **2b** in dichloromethane feature a broad and structureless peak, with a λ_{max} (lifetime; quantum yield) of 537 nm (3.05 ns; 22%) and 642 nm (τ_1 = 0.11 ns, τ_2 = 2.85 ns; <1%), respectively. The emission peaks of **3b** and **4b** in dichloromethane are vibronically structured with a spacing of $\sim$1300 cm^{-1}, in accordance with the C=C and C=N vibrational modes of the naphthyridine moiety. The emission maxima of **3b** and **4b** are almost independent of solvents, while those of **1b** and **2b** are strongly dependent on solvents and shift to the low-energy direction with the increase in solvent polarity (Table S3). The magnitude of the solvatochromic shift is found to depend on the electronic effects of peripheral substituents on the naphthyridine ring. For example, the maxima of the emission spectra of **1b** extend from 448 nm in hexane to 492 nm in toluene and then to 537 nm in dichloromethane. When the electron-withdrawing CF_3 groups are incorporated into the naphthyridine acceptor unit, a more significant solvatochromic shift from 512 nm (in hexane) to 642 nm (in dichloromethane) is achieved in **2b**. In addition, it should be stressed that **1b** and **2b** in polar solvents emit weak fluorescence and display fairly large Stokes shifts (e.g., 97 and 162 nm in dichloromethane, respectively). The spectral dependence of **1b** and **2b** on solvent polarity was further studied on the basis of the Lippert–Mataga equation,[13] and the calculated results reveal an increase of 15.1 and 16.2 D in dipole moment from the ground state to the excited state for **1b** and **2b**, respectively. At this stage, it should be safe to suggest that **1b** and **2b** have a pronounced ICT characteristic of the fluorescent states.[14]

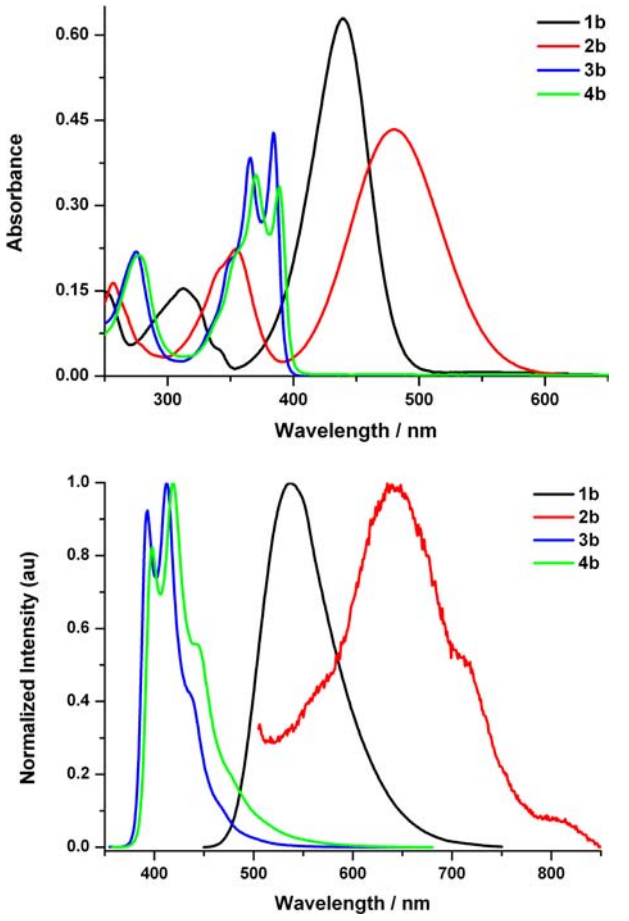

Figure 2. (Top) UV–vis absorption and (bottom) emission spectra of **1b**–**4b** in dichloromethane measured at a concentration of $\sim 1.0 \times 10^{-5}$ mol L^{-1}. λ_{ex} = 440 nm for **1b**, 480 nm for **2b**, and 350 nm for **3b**–**4b**.

Another salient feature for complexes **1b**–**4b** is that their solid-state emissions cover a wide range of 431–670 nm

(12) (a) Zhao, G.-J.; Chen, R.-K.; Sun, M.-T.; Liu, J.-Y.; Li, G.-Y.; Gao, Y.-L.; Han, K.-L.; Yang, X.-C.; Sun, L. *Chem.—Eur. J.* **2008**, *14*, 6935–6947. (b) Grabowski, Z. R.; Rotkiewicz, K.; Rettig, W. *Chem. Rev.* **2003**, *103*, 3899–4032. (c) Demeter, A.; Bürces, T.; Zachariasse, K. A. *J. Phys. Chem. A* **2005**, *109*, 4611–4616. (d) Wilsey, S.; Houk, K. N.; Zewail, A. H. *J. Am. Chem. Soc.* **1999**, *121*, 5772–5786. (e) Ward, M. D. *Chem. Soc. Rev.* **1997**, *26*, 365–375.

(13) (a) Mataga, N.; Kaifu, Y.; Koizumi, M. *Bull. Chem. Soc. Jpn.* **1956**, *29*, 465–470. (b) Liptay, W. In *Dipole Moments and Polarizabilities of Molecules in Excited Electronic State, in Excited States*, Vol. 1; Lim, E. C., Ed.; Academic Press: New York, 1974.

(14) Chen, R.-K.; Zhao, G.-J.; Yang, X.-C.; Jiang, X.; Liu, J.-F.; Tian, H.-N.; Gao, Y.; Liu, X.; Han, K.-L.; Sun, M.-T.; Sun, L.-C. *J. Mol. Struct.* **2008**, *876*, 102–109.

Table 1. Optical Properties of Complexes **1b**–**4b** at 298 K

compd	$\lambda_{abs}{}^{a}$/nm (ε/mol^{-1} dm^3 cm^{-1})	$\lambda_{em}{}^{a}$/nm (τ/ns; Φ)	Stokes shift/ nm	$\lambda_{em}{}^{b}$/nm (τ/ns; Φ)
1b	440 (63030) 313 (15460) 252 (14910)	537 (3.05; 0.22)	97	542 (3.70, 1.06; 0.04)
2b	480 (41050) 355 (21190) 257 (15760)	642 (0.11, 2.85; <0.01)	162	670 (0.81, 2.62; 0.01)
3b	384 (41200) 366 (36870) 275 (19330)	392 (1.40; 0.54)	8	431, 450 (0.42, 2.95; 0.16)
4b	389 (30230) 370 (32010) 277 (18990)	397 (0.53; 0.20)	8	439, 461, 496 (0.50, 1.31; 0.27)

[a] In dichloromethane solution. [b] In solid state. ε = molar extinction coefficient. Φ = fluorescence quantum yield, calculated using quinine sulfate as a standard (Φ = 0.546 in 0.5 mol L^{-1} H_2SO_4). τ = fluorescence lifetime.

(Figure 3), while BODIPY dyes barely exhibit fluorescence in the solid state. The fluorescence maxima for all complexes are red-shifted with respect to corresponding emissions in solution. The fluorescence quantum yields of 0.16 for **3b** and 0.27 for **4b** are remarkably higher than those for **1b** (Φ = 0.04) and **2b** (Φ = 0.01). This possibly originates from the fact that the molecular structure of the latter is more planar compared with that of the former. Usually, high planarity may lead to increasing intermolecular interactions and result in fluorescence quenching.

For better insight into the observed spectroscopic properties of **1b**–**4b**, time-dependent (TD) DFT calculations were performed on these complexes with the Gaussian 03 package.[15] All geometrical structures are optimized at the SCRF(PCM/Bader)-B3LYP/6-311++G(d,p) level, with the single-point energy and molecular orbitals calculated at the TD-DFT(SCRF(PCM/Bader)-B3LYP/6-311++G-(d,p)) level. The calculated values for the maximum absorption wavelengths are in fair agreement with the experimental results. Figure 4 shows the electron distribution of the HOMOs and LUMOs for **1b**–**4b**. Although the HOMO and LUMO densities in **3b** and **4b** are delocalized over the whole molecule, the HOMO and LUMO densities of **1b** and **2b** are mainly located on the dimethylaminophenyl group and naphthridyl-boron moiety, respectively. This result also further confirmed that the ICT process did occur from the donor to the acceptor moiety in the latter.

In summary, we developed novel BF_2 core complexes containing 1,8-naphthyridine building blocks. The synthesized complexes show weak to moderate fluorescence in the solid state. In particular, a large Stokes shift has been achieved for **1b** and **2b** through the introduction of an electron-donating group onto the phenyl ring to construct push–pull-type architecture. The photoinduced intramolecular charge transfer process was analyzed on the basis of the Lippert–Mataga

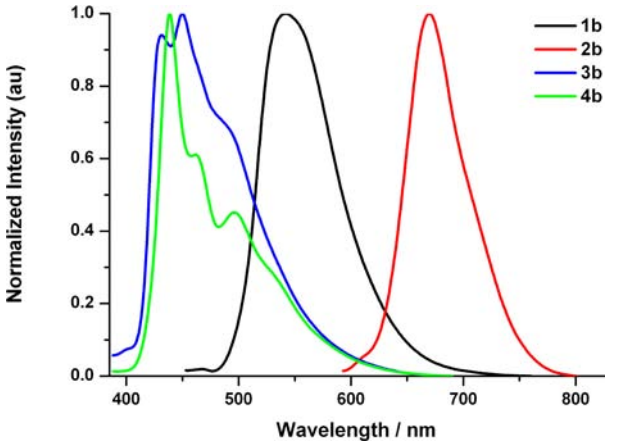

Figure 3. Normalized solid-state emission spectra of **1b**–**4b** at rt (λ_{ex} = 365 nm for **1b**, **3b**, **4b** and 550 nm for **2b**).

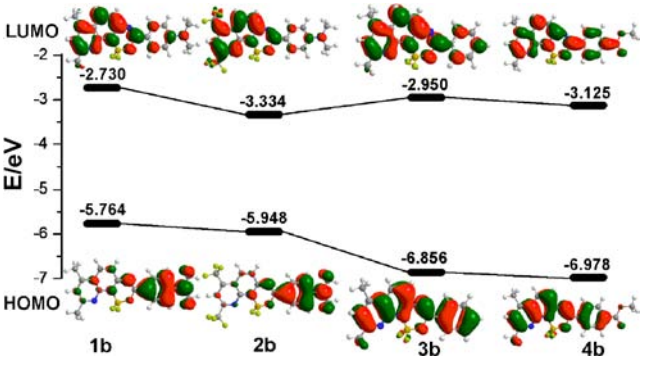

Figure 4. Molecular orbital energy diagrams and isodensity surface plots of the frontier orbitals of **1b**–**4b**.

equation and further confirmed by theoretical calculations. Efforts to improve the solid-state fluorescence quantum yields and thus to pave the way for usage of these complexes as light emitters in optoelectronic devices are currently in progress.

Acknowledgment. We thank the Natural Science Foundation of China (NSFC Grant Nos. 21071123, 21001110, and U1137606), CAS-Croucher Funding Scheme for Joint Laboratories, and Program for Changjiang Scholars and Innovative Research Team in University (IRT0979) for financial support. Y.C. acknowledges Technical Institute of Physics and Chemistry, Chinese Academy of Sciences ("100 Talent" Program) for funding support.

Supporting Information Available. Experimental procedures, characterization data of compounds **1a**–**4a** and **1b**–**4b**, computational details, additional spectral data, crystallographic data (CIF), and complete ref 15. This material is available free of charge via the Internet at http://pubs.acs.org.

(15) Frisch, M. J.; et al. *Gaussian 03*, revision C.02; Gaussian: Wallingford, CT, 2004.

The authors declare no competing financial interest.